# Numerical study on the impact of traffic lane adjustments and low boundary walls on pedestrian exposure to NO2 in street canyons

# Numerical study on the impact of traffic lane adjustments and low boundary walls on pedestrian exposure to $NO_2$ in street canyons

D. Voordeckers[a, *], T. Lauriks[b], D. Baetens[b], T. Ysebaert[b], S. Denys[b], P. Billen[c], T. Tytgat[b], M. Van Acker[a]

[a] Research Group for Urban Development, Department of Architecture, Interior Design and Urban Planning, Faculty of Design Sciences, University of Antwerp
[b] BioGEM, Department of Chemistry and Biochemistry, Faculty of Applied Sciences, University of Antwerp
[c] Research group Sustainable Energy, Air & Water Technology, Department of Bioscience Engineering, Faculty of Science, University of Antwerp
* Correspondence: Dimitri.voordeckers@uantwerpen.be

## Abstract

Mitigating the adverse effects of air pollution, especially on human health, is one of the greater contemporary challenges for cities. Street canyons have herein been identified as bottleneck areas in urbanized environments. Focusing on the necessity of fast-response interventions, strategies to control source-receptor pathways (e.g. implementing low boundary walls (LBWs)) are gaining interest. A potential strategy which is greatly overlooked is the adjustment (reduction or displacement) of traffic lanes in order to increase the distance between source (traffic) and recipient (pedestrians). Within our study, computation fluid dynamics (CFD) is used to simulate the impact of alternations to traffic lanes (whether or not combined with LBWs) on the pedestrian exposure to $NO_2$ for a specific case-study (Belgiëlei, Antwerp) under two prevailing wind directions. The average differences in $NO_2$ concentrations for the entire pedestrian area ranged between +1.0% to -3.6%. On specific locations, reduction up to -8.0% were reached. In case of perpendicular winds, a lateral displacement of all traffic lanes towards the windward facade including LBWs was found most beneficial to reduce pedestrian exposure. LBWs also showed to be efficient in reducing potential adverse effects of lane displacement under less frequent wind directions.

## Keywords

Air pollution, Computational Fluid Dynamics, traffic emission, dispersion, OpenFOAM, street design

## 1. Introduction

Air pollution is proclaimed by the World Health Organization (WHO) as the biggest environmental risk to human health (WHO, 2016). Numerous epidemiological studies have provided evidence of the adverse health effects of outdoor air pollution, linking it to the development of various cardiovascular and respiratory diseases and a high number (around 7 million annually) premature mortalities (Frank & Engelke, 2005; Khomenko et al., 2021; WHO, 2013). In urban environments, the problem of air pollution is exacerbated, as pollutants get trapped and accumulate in the urban canopy layer (the layer of air extending from the ground surface up to the level of the buildings). Due to the increased residential density and human activity, human exposure to air pollutants in these areas is high (Voordeckers et al., 2021b). It is already widely acknowledged that in the urban canopy layer, street canyons (narrow inner urban roads, flanked by a continuous row of high buildings on both sides), as a result of their lack of natural ventilation due to their morphology, identify as hotspots for increased air pollution especially when traffic volumes are high (> 300 vehicles/hour, Voordeckers et al. (2021b)). Considering the severe impact on human health, it is important for authorities to consider fast-response mitigating strategies for air pollution in street canyons to reduce personal exposure.

Based on multiple studies (Jeanjean et al., 2017; McNabola et al., 2013; Voordeckers et al., 2021a) four main strategies to mitigate air pollutions can be derived: (1) a source-based reduction of the quantity of pollution (e.g. congestion charging) and reducing the emission intensity (e.g. carbon tax), (2) dispersing and diluting pollution by improving the natural in-canyon ventilation (e.g. increasing building height variation or building permeability), (3) pollution deposition (e.g. deposition by greenery or photocatalytic materials) and (4) controlling source-receptor pathways (e.g. shielding pedestrians by using low boundary walls). Source-based reduction measures are already widely deployed by cities.(Yang et al., 2016) However, the results of these measures are still inadequate to meet the European legal thresholds and the recently updated WHO air quality guidelines (EEA, 2021). The electrification of the vehicle fleet also holds great potential to reduce exhaust emission. However, the impact of this measure on PM levels (due to the increasing vehicle weight) is found to be less than expected (Timmers & Achten, 2016). It should also be emphasized that this transition will take several years, whereas the severe impact of air pollution on the human health calls for fast-response interventions. Therefore, secondary strategies are gaining more and more interest to amplify the current exhaust-focused strategies.

Improving natural ventilation in street canyons can be achieved by geometrical changes to the morphology of the street such as adjustments to the building height variations (Ming et al., 2018; Park et al., 2020), roof shapes (Huang et al., 2016; Xie et al., 2005), building setbacks (Hassan et al., 2020; Llaguna-Munitxa & Bou-Zeid 2018) and building permeability (van Druenen et al., 2019; Zhang et al., 2020). However, the implementation time of spatial modifications to the street canyon morphology tends to be very slow, highly expensive and requires a detailed understanding of local meteorological conditions (Jeanjean et al., 2017), which makes them less suitable as tools for fast-response interventions. Greenery and photocatalytic materials are known measures to deposit pollutants. However, in case of greenery in street canyons, it is assumed that the impact of aerodynamic changes as a result from the implementation of greenery is stronger than the pollutant removal capacity (Vos et al., 2013). Numerous studies also show high potential for the implementation of photocatalytic materials (e.g. photocatalytic paints) but the effects of photocatalytic oxidation (PCO) are strongly dependent on numerous meteorological conditions such as the amount of sunlight, the pollution intensity and the ventilation rate (Ballari & Brouwers, 2013; Boonen & Beeldens, 2014; Maggos et al., 2008) and it has a high economic cost (e.g. sixty times higher than the planting of trees) due to the short life span and maintenance requirements such as annual cleaning or reapplication (Jeanjean et al., 2017).

Lastly, controlling source-receptor pathways is brought to the fore as an interesting strategy to generate an immediate reduction of the pedestrian exposure to air pollutants. The implementation of low boundary walls (LBWs) to reduce pedestrian exposure is already widely investigated. An idealized study by McNabola et al. (2009) suggests that the implementation of LBWs could reduce pollutant concentrations at respitory height ranging from 40% - 75% depending on the wind direction. A more realistic computational fluid dynamics (CFD) study by Jeanjean et al. (2017), which applies LBWs on a case study (Oxford Street, London, UK), suggests an average $NO_2$ concentration reduction of 2.3% on footpaths and a 23.8% increase on the roadside. In general, LBWs will not reduce the overall in-canyon pollution but, due to aerodynamic effects, pollution is more likely to get trapped on the roadside, exempting the pedestrian area from increased pollution. Roadside barriers also have a rapid implementation process (e.g. recent implementation of Jersey barriers to fortify bike lanes in Manhattan; NYC Department of Transportation (2022)), which makes them eligible as fast-response tool.

Another far less examined tool to reduce pedestrian exposure is the adjustment of traffic lanes, mainly to increase the distance between the source (motorized traffic) and the recipient (pedestrians). Numerous studies have been conducted on changing different variables in street canyons, though only few give guidance regarding source shape and position (Chan et al., 2001; Jicha et al., 2000; Kastner-Klein & Plate, 1999; Liu & Barth, 2002; Tan et al., 2019). Based on an extensive literature search by Voordeckers et al. (2021a) merely one study (Huang et al., 2015) was conducted specifically on the reduction or the lateral displacement of traffic lanes. However, the study by Huang et al. (2015) uses an idealized two-dimensional numerical model under a perpendicular wind direction, neglecting the impact of the built environment and changing wind directions. Therefore, we conducted a study on the potential of traffic lane adjustments applied on a specific case study (Belgiëlei, Antwerp, Belgium) under two different wind directions. Continuing on the study of Jeanjean et al. (2017), the synergetic potential of combining traffic lane alternations with LBWs was further investigated. Temporary adjustments to traffic lanes are nowadays already implemented as tools to rapidly transform car-oriented streets to pedestrian-friendly areas (e.g. the 24 hour transformation of St. Julian Street in Salzburg (Austria), decreasing the number of traffic lanes by half and subsequently creating a larger pedestrian domain (Hauch, 2010)). Our study aims to investigate the potential of these measures to be applied as a fast-response strategy to mitigate the pedestrian exposure to air pollution in street canyons.

## 2. Method

### 2.1 Case study: Belgiëlei, Antwerp

The Belgiëlei is a connecting road located in the city center of Antwerp which links two main artery roads for the city: the "Mechelsesteenweg" and the "Plantin en Moretuslei" (see Fig. 1 a,b). According to the Strategic Spatial Structure Plan for Antwerp (s-RSA) the Belgiëlei identifies as a territorial boulevard due to its typical morphological features such as symmetrical road layout with a central tram line (line 2, 6 and 15 linking outer-city neighborhoods to the central train station), 4 traffic lanes and boulevard trees (City of Antwerp, 2006). The Belgiëlei is dominated by motorized traffic, with on average 52% of all transport consisting of cars and 14% of heavy traffic (Telraam, 2020). Regarding air quality, a previous research by Voordeckers et al. (2021b) points out the Belgiëlei as one of the more problematic street canyons in Antwerp due to its aspect ratio (AR ≈ 0.83) and its high traffic intensity (averagely 310 vehicles per hour and 699 vehicles per hour during rush hours). Also, in 2018, $NO_2$ concentrations were measured in 321 street canyons in the city of Antwerp (Belgium) as part of the large-scale citizen-science project "CurieuzeNeuzen" (De Craemer et al., 2019; Meysman & De Craemer, 2018) pointing out the Belgiëlei as one of the most polluted street canyons in the city of Antwerp with yearly averaged $NO_2$ values ranging between 40 – 55 $\mu g/m^3$. The Belgiëlei is identified as a residential area by the Flemish zoning plan (Geopunt Vlaanderen, 2020) and holds therefore mainly residential functions mixed with some vulnerable functions such as two primary schools, three daycares and functions related to health care. The housing density around the Belgiëlei is a factor 1.7 higher compared to the average housing density in Antwerp (about 90 houses / ha compared to the average in Antwerp of 53.2 houses / ha, City of Antwerp (2021)). With averagely about 1.500 cyclists per day (Telraam, 2020), the Belgiëlei is also an important axis for cyclists to move through the city. In general, it can be concluded that the air quality in the Belgiëlei does not comply with the legal thresholds and that the exposure to air pollutants is high (especially due to the high cyclist activity and increased housing density), emphasizing the necessity of testing fast-response interventions for this case study.

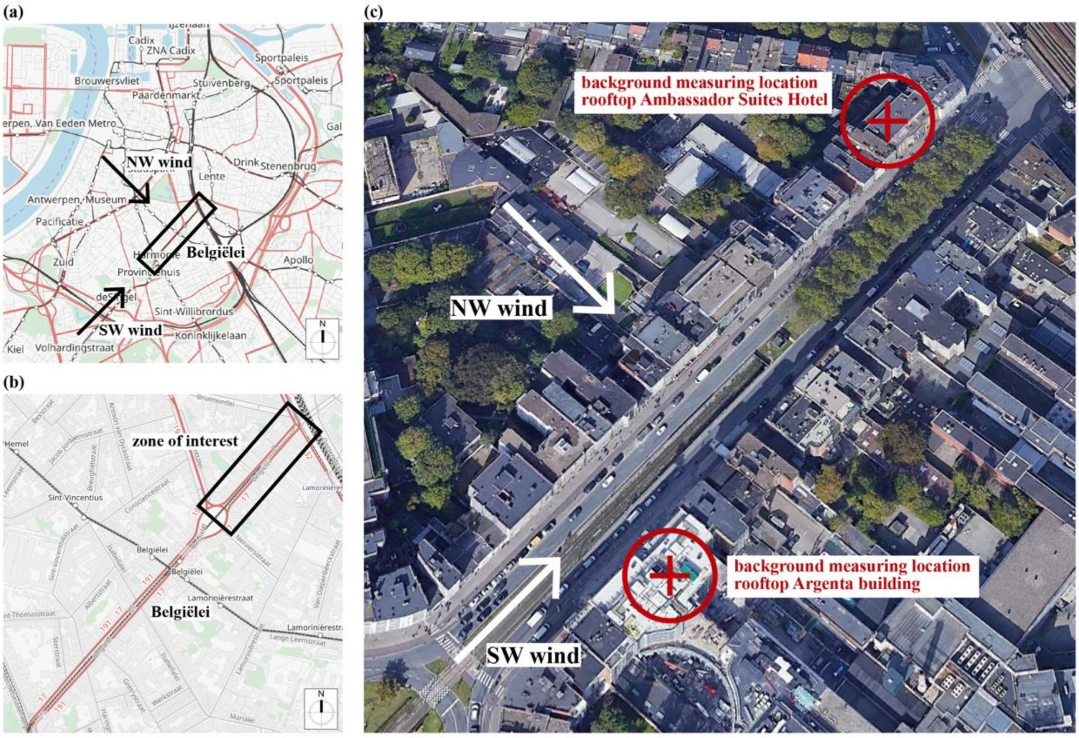


Fig. 1. Location of the area of interest with (a) the location of the Belgiëlei in the city center of Antwerp, (b) the location of the area of interest (northeastern part of the Belgiëlei) and (c) aerial view of the area of interest with the background pollution measuring locations marked in red. The used wind direction (SW and NW) are indicated by arrows in a and c. Retrieved from OpenStreetMap (n.d.) and Google Earth (Google, n.d.).

### 2.1.1 Geometrical street layout

The Belgiëlei has a total length of about 1 km. For the purpose of this research and due to limitations on computational resources , a section of 300 m long was selected in the Northeastern part of the Belgiëlei (see Fig 1b). This section was selected based on the presence of a limited number of variabilities (no intermediate crossroads, no variations in number of lanes, constant street width (36 m) and limited building height variations) which is of great interest for the purpose of this research, since the results of the measurements and the model will be easier to analyze than in a more complicated street section. In addition, e.g. cross roads and more building variation will lead to increased ventilation. Hence, the chosen street section probably represents a worst case scenario and such locations deserve the most urgent attention. Besides, since the chosen location likely represents a worst case scenario, it can be expected that conditions at other locations are equal or less pronounced, i.e. the obtained results will be extrapolatable. Half of the section has boulevard trees (Plantanus Hispanica, City of Antwerp (2022)) and the other half is without trees, making it possible to compare the effect of the implemented measures in both sections. The southwestern section (section without trees) has a descending central tram line, which continuous underground in the northeastern part. In the center of the selected section an air quality measurement station of the Flemish Environmental Agency (VMM) is present. The axis of the street is southwest (or northeast) oriented, parallel to the dominant wind direction (see 2.1.3). For the CFD geometry, building data was retrieved from the 3D model of the City of Antwerp (City of Antwerp, 2022) and missing elements (e.g. all vegetation, traffic lanes and a part of the elevated railroad nearby the zone of interest) were measured on site or estimated via Google Earth and added to the model.

### 2.1.2 Pollutant ($NO_2$) emissions

To quantify the $NO_2$ emissions, vehicle counts were conducted from the 7$^{th}$ of July 2021 to the 6$^{th}$ of September 2021 in the selected section of the Belgiëlei using two (one for each driving direction) MetroCount® MC5900 devices (MetroCount, 2015). Analogously to the work of Blocken et al. (2016) and Lauriks et al. (2021), the conversion of vehicle numbers per time unit [$T^{-1}$] to pollutant emissions [M $T^{-1}$] was conducted by subdividing the traffic in traffic types (cars, buses, light and heavy trucks) and using emission factors [M $L^{-1}$] for fluent urban traffic of the Dutch government (Rijksoverheid, 2021). For the purpose of our research, average traffic intensities during rush hours (17h00 – 18h00) were used and traffic emissions were hereby set to 6.62x$10^{-7}$ kg $s^{-1}$ for the southwestbound lane and 7.04x$10^{-7}$ kg $s^{-1}$ for the northeastbound lane. Similarly to Blocken et al. (2016), traffic emissions were released from volumes (cuboids of height 1.5 m and width 2 m) attempting to resemble turbulent mixing caused by the air displacement of passing vehicles. On-site observations showed that, rather than following the two-by-two traffic lane layout, drivers tend to drive in the middle of the 2 lanes and at the end of each direction, nearby the traffic lights, they convert back to two lanes and traffic stagnates (see Fig. 4a). Therefore, emission volumes were placed in the center of the road and at the end of each road, at a distance of 69.5 m (measured on site) in front of the traffic lights, the volumes were split in two and emission factors for stagnating traffic were used (3.60$e^{-7}$ kg $s^{-1}$ (southwestbound) and 3.81x$10^{-7}$ kg $s^{-1}$ (northeastbound)). The increased emissions were calculated by using the emission factors for "city stagnating" traffic by data from Rijksoverheid (2021). A detailed overview of the used emission factors and mass flow rates can be found in Appendix A. Similar to Jeanjean et al. (2017), the $NO_2$ emissions are modelled as non-reactive since it can be assumed that this does not significantly affect the spatial distribution and errors will be limited (<15% based on Santiago et al. (2017), see Section 3.4). Thermal effects can also affect the dispersion of gaseous pollutants, however, previous studies (Parra et al., 2010; Santiago et al., 2017) have indicated that wind dynamics are predominant over thermal effects in case of high wind speeds (> 2 m $s^{-1}$). The used wind speeds are approximately 4.5 m $s^{-1}$ (see 2.1.3), justifying the neglection of thermal effects (isothermal flow).

### 2.1.3 Background conditions

To determine the meteorological conditions, wind speed and direction were measured from the 7$^{th}$ of July 2021 to the 14$^{th}$ of September 2021 at a height of 40 m (by placing a meteo mast of 12 m in height on a 38 m high rooftop of the Argenta Building in the zone of interest; Fig. 1c) equipped with an ORA wind speed and wind direction sensor (Lambrecht Meteo, n.d.). Due to time limitations, unlike the study of Jeanjean et al. (2017), no weighted average was calculated from all possible wind directions. Instead, two important wind directions were selected. They were both analysed as separate scenarios and merged together as weighted averages, based on the frequency of occurrence of the concerning wind direction. In order to determine which wind directions to use for the scenarios, it was calculated from the measurements that SW - being parallel to the length axis of the studied street section - is the prevailing wind direction (14.0% of all wind measurements when divided into 16 wind directions). The second wind direction that was used is NW, which is perpendicular to the length axis. This direction is not the second most occurring, but still rather frequent, 9.2% of all observations. It was selected as second wind direction, because wind perpendicular to the length axis is probably the least favorable condition for air pollution (Voordeckers et al., 2021a). The second direction hence likely represents a worst case scenario. Besides, the intention of this study is analyzing the conditions during rush hour (17h00 – 18h00), when air pollutions levels will be at their worst. In the wind measurements, it was observed that it frequently occurs that the wind direction is (approx.) constant for one hour or more. Parra et al. (2010) demonstrated that steady RANS can be used to reasonably accurately calculate dispersion results averaged over one hour. Hence, it will frequently occur in reality that both selected wind directions are constant during the selected rush hour and these conditions can be reasonably accurately modelled using steady RANS. For both wind directions the corresponding measured average wind speeds (u_ref) were 4.59 m $s^{-1}$ (SW) and 4.49 m $s^{-1}$ (NW). Subsequently, the same meteo mast was used to measure $NO_2$ background concentration (using a $NO_2$-B43F sensor (Alphasense, 2022), calibrated at the VMM station at the Belgiëlei) for the SW scenario. For the NW scenario, the background concentration was measured with a sensor placed at the rooftop of the Ambassador Suites Hotel (NW side of the Belgiëlei, see Fig. 1c). For the selected wind directions, average background concentrations of 27.83 ± 2.7 µg $m^{-3}$ (SW) and 25.58 ± 5.1 µg $m^{-3}$ (NW) were measured (error is SEM).

## 2.2 CFD model

### 2.2.1 Governing equations

Simulations were performed using OpenFOAM v8 (OpenFOAM, 2022). The incompressible steady Reynolds-Averaged Navier Stokes (RANS) equations were solved, where the system of equations was closed using the k - ε turbulence model. The k - ε model was selected because in OpenFOAM v8 it is intended to be used in conjunction with the available atmospheric boundary layer inlet boundary conditions (OpenFOAM, n.d.). Pollutant transport was simulated by adding a scalar transport equation wherein the standard gradient diffusion hypotheses was applied, with a turbulent Schmidt number ($Sc_t$) value of 0.75 (mean of the range 0.2-1.3 in which $Sc_t$ usually varies in atmospheric dispersion as described by Tominaga and Stathopoulos (2007)).

### 2.2.2 Computational domain and mesh

The dimensions of the computational domain were determined in accordance with the guidelines of Franke et al. (2007). Buildings surrounding the zone of interest were explicitly represented, if their distance from the zone of interest was smaller than 6 times their height. The vertical extension of the domain was set to $6H_n$, with $H_n$ being the height of the tallest building (59.8 m). In all horizontal directions, the boundaries of the domain were set at a distance of $15H_n$ of the explicitly modelled buildings since multiple wind directions are used, thus all boundaries have to be able to serve as outflow for the computational domain. Buildings present in the computational domain which are not explicitly represented (e.g. in the approach flow zone) were also taken into account using a rough wall function (see 2.2.3).

Concerning the grid, it was tried to perform a grid convergence check. Grid convergence was not fully reached. The cause was probably that the simulation had to be stabilized by using first order discretization for the convection of the turbulence variables, k and ε, and a total variation diminishing scheme for the convection of the other variables. The used grid seemed to have at least a reasonable resolution and the solution did not change qualitatively by using a finer grid. A uniform hexahedral base mesh was constructed in blockMesh, where all cell sides measured 6.7 m. Subsequently, refinements were made using snappyHexMesh in the following mesh parts: The entire part of the domain from 0 to 5 m was refined twice, from 5 to 10 m once. A rectangular box was placed on the bottom plane and over the buildings. The horizontal distance between the buildings and the box was at least 130 m. The height of the box was 70 m. One refinement was made inside this box. A similar box was placed inside the former box, with a height of 50 m and a minimal horizontal distance from the buildings of 65 m. Two refinements were made inside the second box. (The height of many buildings was approx. 30 m.) Refinements were made up to a certain distance from the buildings and the part of the bottom plane containing the Belgiëlei: up to 1.25 m was refined 4 times, up to 5 m 3 times. Finally, inside the volumes of the trees and pollutant sources, 3 refinements were made. All refinement levels are expressed relative to the base mesh. The average cell sizes on the buildings and Belgiëlei road plane was hence 0.42 m. This resolution allowed more than 10 cells to be present across the street in the zone of interest, ensuring proper flow modelling (Jeanjean et al., 2017). In total, the grid consists of approximately 69.3 million cells.

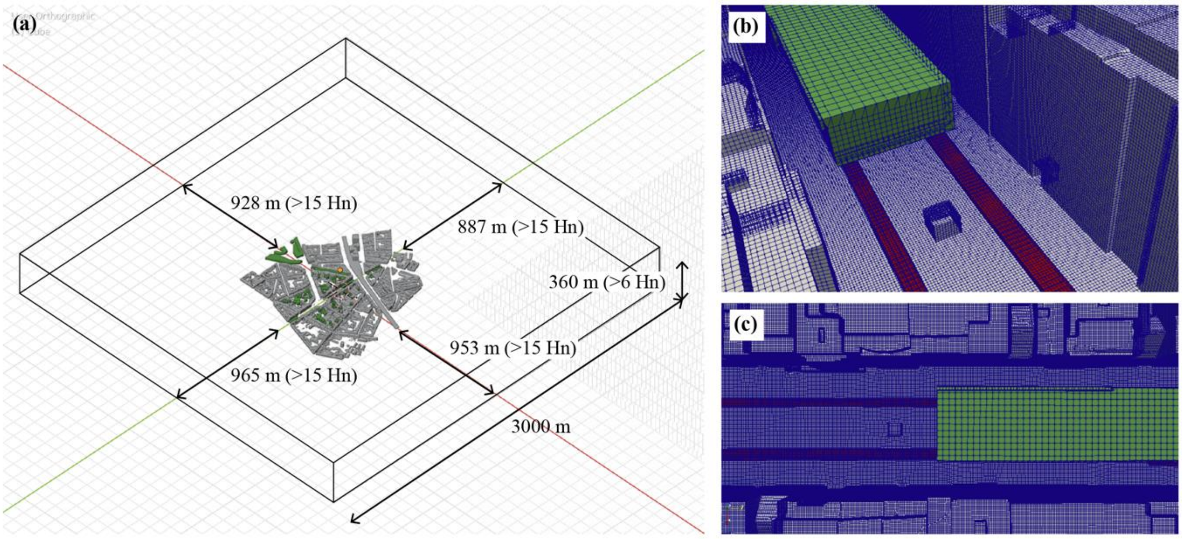


Fig 2. Computational domain and mesh with (a) the implicitly modelled area inside the full domain and (b,c) a visualization of the used mesh to carry out CFD simulations with (b) a 3 dimensional view and (c) a top view.

### 2.2.3 Boundary conditions and flow calculation

A slip boundary condition was applied at the top of the domain and the vertical boundaries were set in pairs as outlet (p set to constant static pressure and the other variables to zero gradient) or inlet, as required for the corresponding wind direction. To all the buildings and streets surrounding the zone of interest, a smooth wall function was applied. Within the zone of interest, the street surface was drawn as a smooth surface and various small obstacles (e.g. benches or bicycle stands) were taken into account by applying a rough wall function with $z_0$ = 0.25 based on the revised Davenport roughness classification (Wieringa, 1992). A rough wall function with $z_0$ = 2 was set for the bottom part of the domain where buildings were not explicitly represented. At the inflow boundaries, the average streamwise velocity ($\langle u \rangle$), the turbulent kinetic energy (k) and the turbulence dissipation rate ($\epsilon$) were specified by the following equations:

$$\langle \boldsymbol{u} \rangle = \frac{\boldsymbol{u_*}}{\boldsymbol{\kappa}} \boldsymbol{ln}\left(\frac{\boldsymbol{z} + \boldsymbol{z_0}}{\boldsymbol{z_0}}\right) \tag{1}$$

$$k = \frac{u_*^2}{\sqrt{C_\mu}} \tag{2}$$

$$\epsilon = \frac{(u_*)^3}{\kappa(z + z_0)} \tag{3}$$

where $u_*$ is the friction velocity, $\kappa \approx 0.41$ is the von Karman constant, z is the height coordinate (m), $z_0$ is the roughness length and $C_\mu$ a constant equal to 0.09 (Gromke & Blocken, 2015). For the wind flow calculation, a residual convergence of at least $10^{-4}$ was reached for all variables. For the scalar transport simulation, a residual convergence of $10^{-6}$ was reached. The simulation time per wind direction was 32 hours on average using 336 cores.

### 2.2.4 Vegetation modeling

Within the zone of interest, 2 rows of 11 London plane trees (Platanus × hispanica) are present. To simplify the model, the parameters derived for the London plane trees were applied on all vegetation. Vegetation was implicitly represented as a uniform porous medium, where tree crowns were represented as cuboids or cylinders. Tree trunks were not included. The influence of the vegetation was modeled by adding source terms (only active in the computational vegetation cells) in the momentum (Eq. 4), turbulence (Eqs. 5 and 6) and pollutant transport (Eq. 7) equations (Buccolieri et al., 2018; Gromke & Blocken, 2015; Katul et al., 2004; Moradpour et al., 2017; Sanz, 2003):

$$S_{u_i} = -\rho \cdot \mathrm{LAD} \cdot C_d U_{u_i} \qquad [\mathrm{Pa\,m^{-1}}] \tag{4}$$

$$S_k = \rho \cdot \mathrm{LAD} \cdot C_d\left(\beta_p U^3 - \beta_d U k\right) \qquad [\mathrm{kg\,m^{-1}s^{-3}}] \tag{5}$$

$$S_\varepsilon = \rho \cdot \mathrm{LAD} \cdot C_d(C_{\varepsilon 4}\beta_p \frac{\varepsilon}{k} U^3 - C_{\varepsilon 5}\beta_d U \varepsilon) \qquad [\mathrm{kg\,m^{-1}s^{-4}}] \tag{6}$$

$$F_d = -\mathrm{LAD} \cdot \mathrm{v_d} \cdot c \qquad [\mathrm{kg\,m^{-3}s^{-1}}] \tag{7}$$

where $\rho$ is the density of air, LAD [$m^2$ $m^{-3}$] the leaf area density, $C_d$ [-] the leaf drag coefficient, $U$ the velocity magnitude, $u_i$ the velocity component of direction i, $\beta_p$ the fraction of mean kinetic energy that is converted into wake turbulent kinetic energy by means of drag, $\beta_d$ a dimensionless coefficient representing the short-circuiting mechanism of the turbulence cascade, $C_{\varepsilon 4}$ and $C_{\varepsilon 5}$ are empirical coefficients, $v_d$ [m $s^{-1}$] is the deposition velocity, and $c$ [kg $m^{-3}$] is the pollutant concentration. LAD was set at 1.6 based on previous research on London plane trees by Hofman and Samson (2014). $C_d$ was adopted from Gromke and Blocken (2015) and set to 0.2. Based on the work of Sanz (2003) and Katul et al. (2004), $C_{\varepsilon 4}$ and $C_{\varepsilon 5}$ were set to 0.9, $\beta_p$ to 1.0 and $\beta_d$ to 5.1. In accordance with values described by both Santiago et al. (2017) and Lovett (1994) a value of 0.005 m $s^{-1}$ was selected for $v_d$.

### 2.2.5 Comparison between model results and on-site measurements

The results of the baseline model (base scenario or current state) were compared to on-site $NO_2$ measurements. To do so, a measuring campaign was conducted from the 6th of July 2021 until the 9th of August 2021. Ten low-cost sensors ($NO_2$-B43F sensor) were used, of which eight were placed inside the street canyon and two (sensor 9 and 10 in Fig. 3) on top of the two highest buildings in the zone of interest in order to estimate the background concentration (campaign setup see Appendix B). $NO_2$ was measured on a five-minute frequency and converted to hourly averages. The measuring station of the Flemish Environment Agency (VMM), located in the middle of the Belgiëlei, was used to calibrate the $NO_2$ sensors. The background wind direction was measured by a meteo mast (10 m in height) which was placed on top of the highest building in the Belgiëlei (Argenta building). For each $NO_2$ sensor, the standard deviation was calculated. The average standard deviation, 6.5 µg $m^{-3}$, was used as measurement error.

Subsequently, the measured data which was collected under the same conditions as the baseline model (NW and SW wind direction during rush hour) were selected to conduct the comparison between the model output and the measured $NO_2$ values (visualized in Fig. 3). In general, the model underpredicted the $NO_2$ values with a mean bias of -6% (-2.2 µg m-3) under SW winds and -17% (-6.3 µg $m^{-3}$) under NW winds. Based on the requirements formulated by Chang and Hanna (2004), the model performance can be described as “good” since (1) all model predictions are within a factor two of the observations, (2) the mean bias is within ± 30% of the mean and (3) the random scatter is less than a factor of two of the mean (a factor ≈1.3 under SW winds and a factor ≈1.6 under NW winds). Figure 3c represents a “fractional bias (FB) versus normalized mean square error (NMSE)” plot, which is often used as a plot to indicate the overall relative model performance (Chang & Hanna, 2004). For the SW and NW models, NMSE and FB are close to zero and within the parabola which represents the minimum NMSE for a give FB, indicating a good model performance. The “FB versus NMSE” plot confirms the slight underprediction (FB = 0.08 for SW and FB = 0.22 for NW) of the models. In general, it can be concluded that the model is suitable for the purpose of the current research. However, a more detailed model validation is suggested for the purpose of additional research.

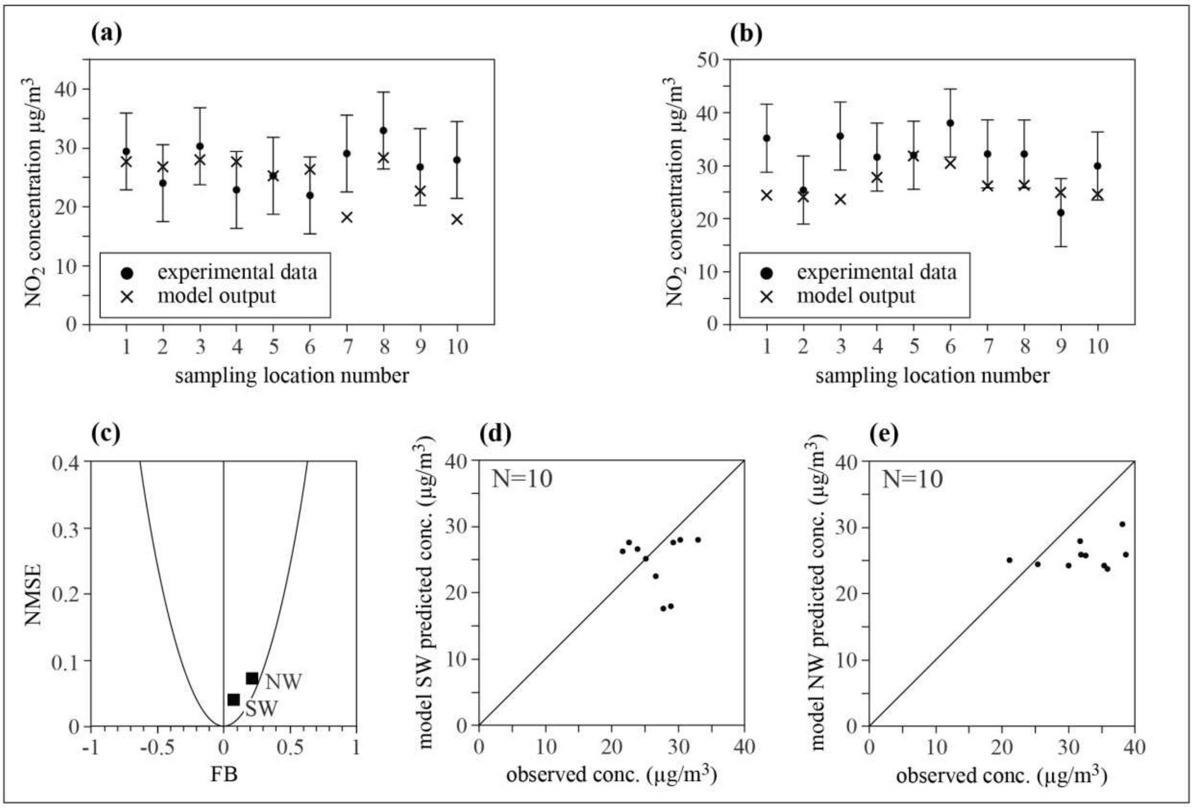


Fig 3. Comparison between model results and on-site observations with: (a,b) plots of the measured and modelled $NO_2$ concentration on the sampling locations with (a) the data for the model under SW winds and (b) the data for the model under NW winds; (c) "fractional bias (FB) versus normalized mean square error (NMSE)" plot with the parabola indicating the minimum NMSE for a given FB and (d,e) scatter plots of the observed and predicted concentrations with an indication of the number of points (N) in each frame, with (d) the scatter plot for the SW model and (e) the scatter plot for the NW model. $NO_2$ concentrations are presented in µg m$^{-3}$.

## 2.3. Fast-response mitigation strategies

All scenarios are visualized in Fig. 4. In total, 7 scenarios were simulated under two wind directions (SW and NW resulting in 14 simulations in total): (1) the current state (scenario 0), (2,3) scenario 1 with a lane reduction with and without LBWs, (4,5) scenario 2 with a southeast lateral lane displacement with and without LBWs and (6,7) scenario 3 with a northwest lateral lane displacement with and without LBWs. For the first scenario, the double traffic lanes (which are currently used as a single driving lane with cars driving in the middle of two lanes) are converted to single traffic lanes with the minimal required width (for emergency access) of 4 m (City of Antwerp, n.d.). The traffic lanes were placed as close as possible to the central axis of the road, in order to maximize the distance towards the current pedestrian area (increased distance of 1.80 m). At the end of each driving direction (in front of the traffic lights) traffic lanes were split again over a distance of 69.5 m, analogously to scenario 0. In case of scenario 2 and 3, single direction traffic lanes were converted to two way lanes, using the currently available street width (7.0 m at the southeastern side and 7.30 m at the northwestern side). Due to the lack of space, traffic lanes were not split in front of the traffic lights, but the length of the cuboid representing stagnating traffic was increased (69.5 m to 110 m), since it is presumable that more stagnating traffic will appear in front of the traffic lights due to the reduction of traffic lanes. All scenarios were simulated once without LBWs and once with LBWs. The LBWs have a height of 1.2 m, a width of 0.6 m and were placed as close to the roadside as possible, following the guidelines of Voordeckers et al. (2021a). However, where possible, additional street width for the purpose of parallel parking was left on the right side of the road in every driving direction. Also, LBWs were cut at specific locations for accessibility reasons (e.g. entrance parking or private garage). The interventions are site-specific but also represent a more realistic application of LBWs in a street canyon. Lastly, it should be emphasized that in reality, a service road should be implemented in the pedestrian area for S02 and S03, to ensure accessibility for all buildings. However, potential additional emissions due to sporadic traffic on this service road were neglected in our study.

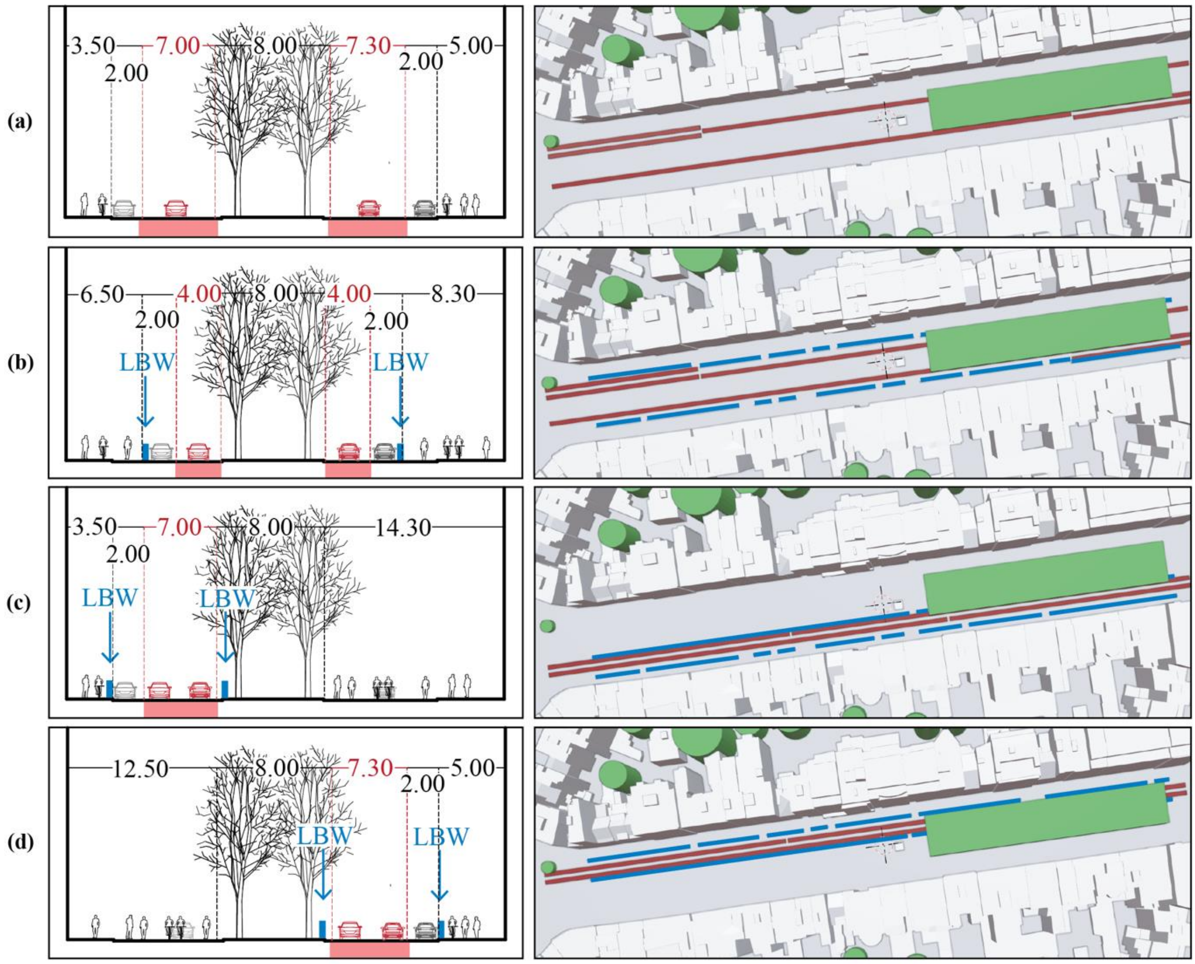


Fig 4. Visualization of the scenarios as cross-sectional and aerial view with (a) the base scenario (current state), (b) scenario 1 with reduced traffic lanes, (c) scenario 2 with the traffic lanes laterally displaced to the southeast and (d) scenario 3 with the traffic lanes laterally displaced to the northwest. All scenarios are simulated with and without low boundary walls (LBWs). Greenery is visualized in green, the source position in red, parked cars in grey and the LBWs in blue, dimensions are in meters.

# 3. Results and discussion

## 3.1 General performance of the mitigating measures

The simulated $NO_2$ data was gathered out of two sampling zones (cuboids of 1.5 m high, 2 m wide and 260 m long in front of the facades on both sides of the road) representing the pedestrian respiration zone, in which the average $NO_2$ value within each grid cell (> 65.000 grid cells for both sampling zones) was collected and used for further analysis. The gathered $NO_2$ concentrations for every scenario in both applied wind directions (NW and SW) are represented in Fig. 5. Comparing the data between both wind directions clearly shows a strong difference in the interquartile ranges (IQR), suggesting that for the SW wind direction (parallel) the $NO_2$ concentration is more evenly distributed. Scenarios 1 and 2 (with and without LBW) resulted in a reduction of the $NO_2$ concentrations in the respiratory zones. S03 was the only scenario resulting in increased average $NO_2$ concentrations (see averages marked with X in the boxplots of Fig. 5). The weighted average (based on the frequency of the NW and SW wind directions) reductions for the scenarios are the following: -0.8% for S01, -1.3% for S01 including LBWs, -3.2% for S02, -3.6% for S02 including LBS, +1.0% for S03 and -0.8% for S03 including LBWs. The reduced $NO_2$ concentrations for S02 and increased concentrations for S03, especially under NW wind conditions, can easily be explained by appearance of a so called "skimming flow" (Oke, 1988) and the hereby developed in-canyon vortex, transporting the pollution to the leeward facade of the street canyon (see Fig. 7c). It is therefore possible that in case of a SE wind direction, an inverted vortex will appear, reversing the results of S02 and S03. However, during the field research, the frequency of SE winds was only 2.1%. Additional reductions by implementing LBWs were found to be substantial, with an additional relative reduction percentage of 63.0% for S01, 13.5% for S02 and 182.4% for S03 based on the weighted average reductions. The largest relative change in reduction was found for S01 under NW winds (613.7%). When comparing the relative reduction percentages, it can be concluded that the efficiency of LBWs is generally higher under perpendicular (NW) wind conditions (relative change in reduction percentage of 613.7% for S01, 12.2% for S02 and 89.1% for S03 under NW winds and 42.1% for S01, 18.5% for S02 and 52.0% for S03 under SW winds). Only for S02 LBWs were found to be slightly more efficient under NW wind conditions. This can be explained by the fact that, in case of NW winds, the LBWs are placed in the windward area of the in-canyon vortex, where the increased wind speed of the downdraft of the vortex transports the pollution over the LBW (see Fig. 7b). A potential solution to this phenomenon is to increase the height of the LBW on the NW side of the street, containing the pollution again on the roadside. However, further research should be conducted on this matter.

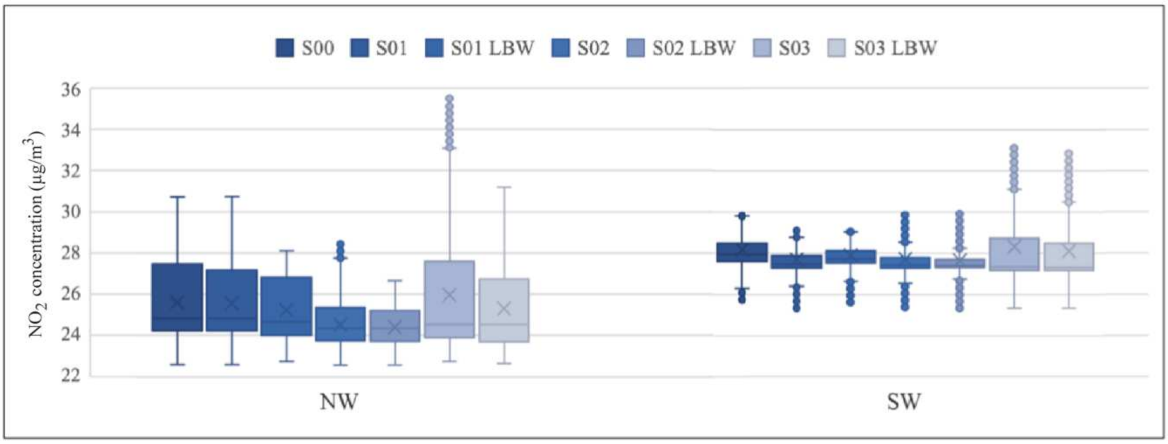


Fig 5. Data visualization of the simulated $NO_2$ concentrations in the pedestrian respiration zone for the prevailing wind directions (NW and SW) for the base scenario (S00), the scenario proposing a lane reduction (S01), the scenario proposing a lateral lane displacement towards the southeastern side of the Belgiëlei (S02) and the scenario proposing a lateral lane displacement towards the northwestern side of the Belgiëlei (S03). All scenarios were modelled with and without low boundary walls (LBW).

### 3.2 Site-specific differences

To get more profound insights on the performance of the mitigating measures the previous sampling zone was subdivided into 4 subregions depending on their spatial features (2 zones in the area with trees, one on the NW side of the road and one on the SE side of the road and 2 zones in the area without trees, divided similarly. The $NO_2$ changes were hereafter compared for all the scenarios in all the subregions (results see Fig. 6).

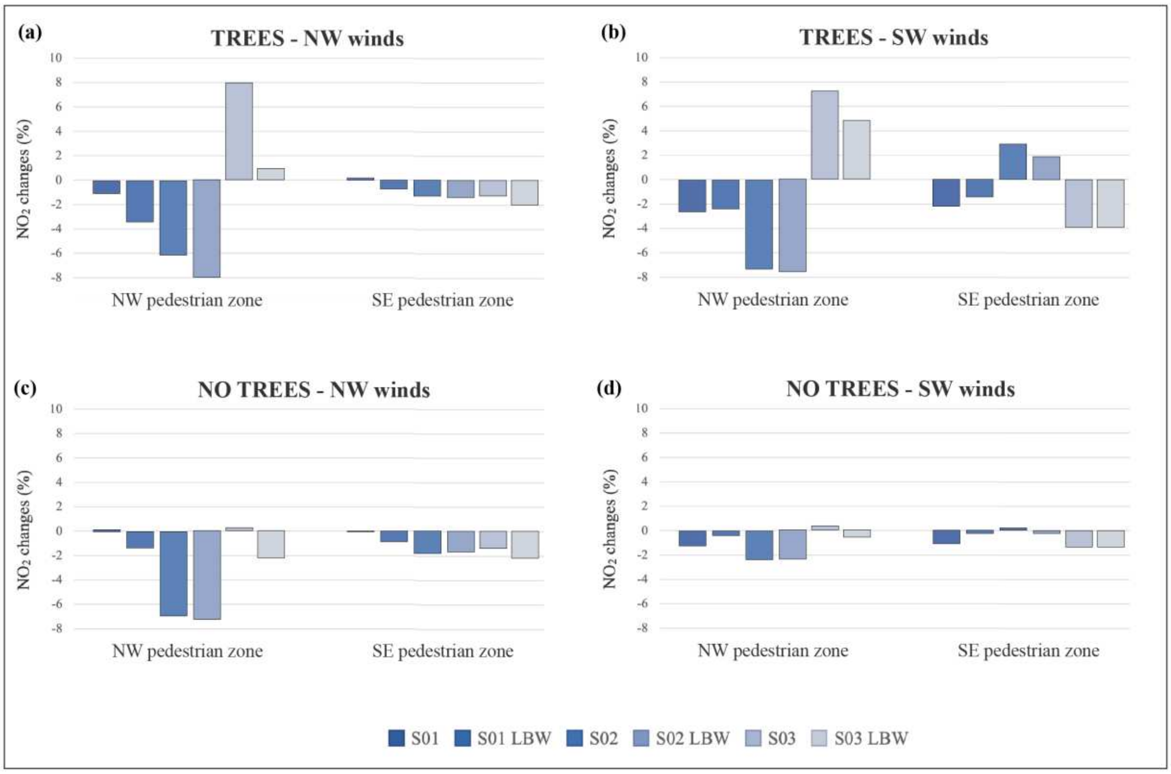


Fig 6. Simulated average $NO_2$ reductions for every scenario for 4 different sampling zones (2 on both sides of the street canyon in the area with trees and 2 in the area without trees) and for both prevailing wind directions (NW and SW).

The lateral displacement of the traffic lanes towards the southeast side of the Belgiëlei combined with LBWs (S02 LBW) seems most favorable to reduce pedestrian exposure to $NO_2$, especially for the NW pedestrian zone (average reductions ranging from -2.3% to -8.0%). Only in the area with trees, an average increase of $NO_2$ concentration of 2.9% is observed in the SE pedestrian area. In contrast to these finding, the lateral displacement of the traffic lanes towards the northwestern side of the Belgiëlei (S03) has an explicit negative effect in the area with trees, with average increases up to 8.0% . The usage of LBWs mitigates this effect to some extent, as expected, but does still result in a substantial increased exposure compared to the base scenario. The first scenario (lane reduction) has a more modest impact on the $NO_2$ concentrations, with average changes ranging from +0.1% to -2.4%. Therefore, it can be concluded that this scenario in reality will likely have a (modest) positive effect on the pedestrian exposure to $NO_2$ emitted by local traffic, regardless of the wind direction or the presence of trees. Besides, combining the lane reduction with LBWs was observed to improve the effectiveness in general (Section 3.1). However, it also reduces the effectiveness at all the subregions in case of SW winds (see Fig. 6 b,d). Finally, Fig 6 a,c shows that under NW wind conditions, S01 and S02 are more efficient in reducing $NO_2$ concentrations at the NW pedestrian zone compared to the SE pedestrian zone, and vice versa for S03. This again can be explained by the in-canyon vortex structure, dispersing pollutants towards the leeward facade (see Fig 7 a,b,c). Also, different behavior of the scenarios can be observed in the areas with or without trees. Under SW wind conditions, differences in $NO_2$ change were far more explicit in the area with trees. This can be explained by the fact that pollutants accumulate in this area due to the channeling in-canyon flow with reduced wind speeds at the NE end of the street canyon (Huang et al., 2019), transporting pollution from the SW side towards the NE side (area with trees) of the Belgiëlei, and also due to the presence of the trees, further reducing the local wind speed (Vos et al., 2013). The increased pollution concentrations and/or reduced wind speeds might exaggerate the effect of the interventions. Under NW wind conditions, no large differences in performance were found for S01 and S02 in the areas with or without trees. Only for S03, large differences were observed influence by the presence of trees (see Fig. 7 c,f). Once again, this can be explained by the in-canyon vortex structure, whereas the trees reduce the updraft of the wind, limiting the upward pollution dispersion.

To investigate the large differences in performance of S02 (LBW) and S03 (LBW) the $NO_2$ dispersion patterns were visualized for two sections of the Belgiëlei (with trees and without trees, see Fig. 7). In case of NW wind (perpendicular to the street axis) the dispersion patterns are clearly driven by an in-canyon vortex wind flow (Fig, 7 a,b,c), as described by Oke et al. (2017). Concerning S02 LBW, recall that the traffic lanes are moved closer to the SE pedestrian area. In case of NW wind, however, it is clear that there is no convective transport of the pollutant towards the SE pedestrian area due to the vortex. In addition, the traffic lanes are located further from the NW pedestrian area and it is clear that the pollutants are diluted substantially before they can reach this area. Conversely, in S03 LBW, the traffic lanes are moved closer to the NW area and the vortex is transporting the pollutant directly towards this area. Consequently Fig. 7c demonstrates that under NW winds, S03 LBW results in increased pollution levels at the NW pedestrian area (on average +8.0% without LBW or +0.9% with LBW). However, it also safeguards a large portion of the entire street section (entire region from the street axis to the SE pedestrian zone), since the vortex transports the pollutant away from this area. Fig 7 d,e,f also clearly illustrates the increased effectiveness of the LBWs under SW wind conditions, where the channeling flow combined with the presence of LBWs results in the accumulation of pollutants on the roadside area, limiting the dilution and dispersion of the pollutants in the other parts of the street canyon.

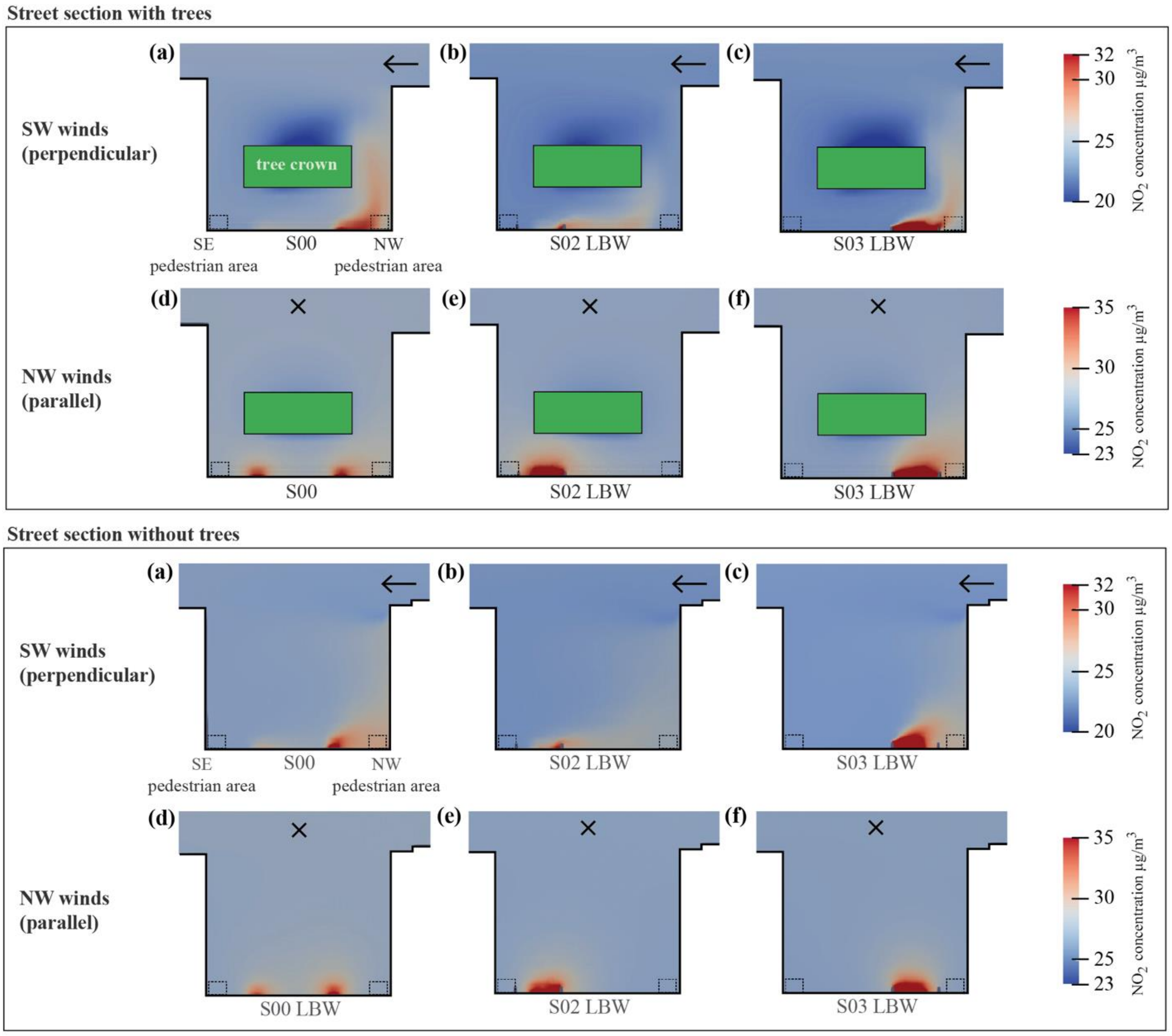


Fig 7. Section of the simulated $NO_2$ concentrations in the zones of interest with trees and without trees for (a and d) scenario 0 (S00), (b and e) scenario 2 with low boundary walls (S02 LBW) and (c and f) scenario 3 with LBWs (S03 LBW) for both selected wind directions (NW and SW).

### 3.3 Guidelines for urban planning

Previous findings can be used to derive a number of general guidelines applicable for urban planning:

- A “classic” boulevard typology might facilitate increased pedestrian exposure to pollutants emitted by local traffic and it might be beneficial to differ from the typical symmetrical street layout. The bundling of traffic lanes on one or the other side of the road might hereby be a useful tool to alter source-receptor pathways.
- Traffic lanes at a wide distance from each other should be avoided. Even in case of an increase in stagnating traffic (which was included in the scenarios, see 2.1.2) the exposure to $NO_2$ was generally reduced by bundling / reducing traffic lanes (S01 and S02).
- The most desirable position of traffic lanes is dependent on the prevailing wind direction. Generally, it can be concluded that for street canyons under perpendicular wind directions a lateral displacements of the traffic lanes towards the windward facade is recommended. However, in any case, a profound analysis of the performance of this measure for multiple wind directions is recommended.
- Low boundary walls can be used as an efficient tool to further reduce exposure to traffic-related air pollution. Also, LBWs can reduce to adverse effect of lane displacements when less frequent wind directions occur (for example to mitigate to expected increase in $NO_2$ exposure for S02 under SE wind directions).

In case of the Belgiëlei and the analyzed wind directions, the lateral displacement of all traffic lanes towards the SE (windward) facade is most effective in reducing $NO_2$ concentrations in the pedestrian areas. However, with regards to urban planning, it should be emphasized that $NO_2$ will still be dispersed in the central area of the street (see central zone marked in red in Fig. 8), especially when a NW wind is present. Based on this finding it is recommended not to use the central zone for human activities (e.g. playgrounds) but rather to use it as a (green) buffer area (see suggestions Spirn (1986)). Also, since traffic volumes are combined, on road $NO_2$ concentrations will increase. Therefore, it is recommended not to allow cyclists on the road because of the increased exposure, but rather to facilitate bike lanes in the safeguarded pedestrian areas. In case of the Belgiëlei, the bike lanes are already present in the defined pedestrian zones.

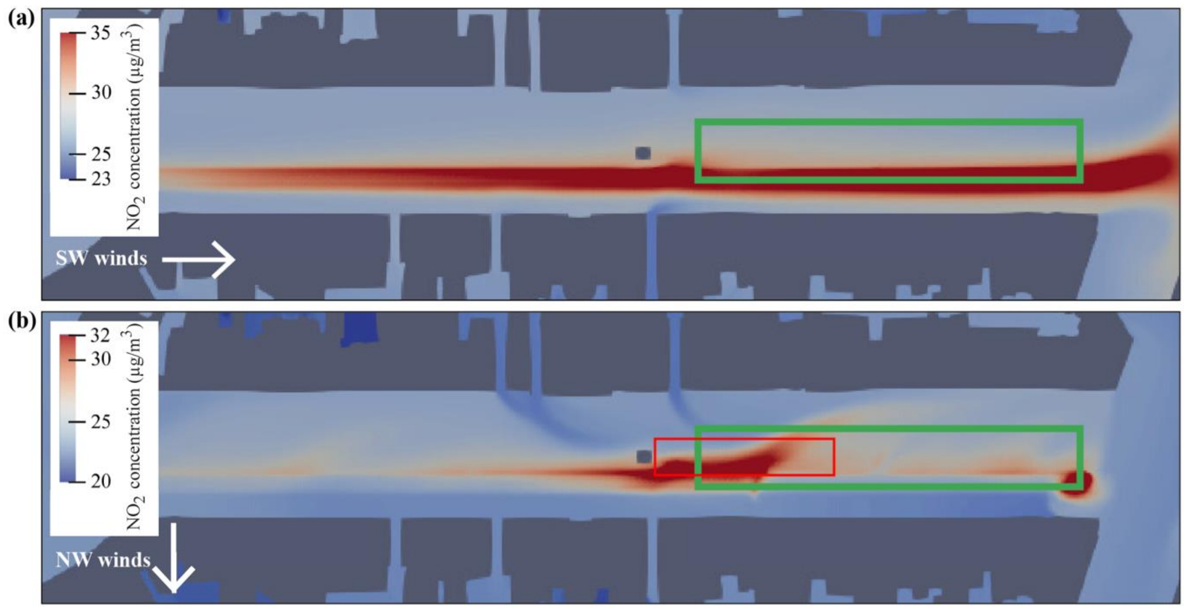


Fig 8. Horizontal section at respiration height (1.5 m) showing the simulated $NO_2$ concentrations in the zone of interest for a lateral displacement of traffic lanes (S02 LBW) for a SW (a) and NW (b) wind direction. The area with trees is marked in green. The area with peak pollutions at the central area of the street canyon is marked in red.

Focusing on the aspect of urban planning, it should also be emphasized that altering the traffic lane composition might be beneficial for numerous other aspects besides pedestrian pollutant exposure. By compressing the amount of space for cars their dominant impact on the public domain is diminished, which creates opportunities to increase livability (wider pedestrian areas, larger social areas), safety (bundled traffic lanes separated from pedestrians and cyclist) and potentially even ecological values (increasing plant variety in buffer zones or creating water detention areas). This might transform current traffic-dominated boulevards into multi-functional structures and restore their structuralizing character within urban environments.

### 3.4 Limitations and uncertainties

In any study regarding air quality in urban environments, a high number of variabilities is present, which is an inherent characteristic of real-world atmospheric conditions (Neophytou et al., 2011; Voordeckers et al., 2021a). This introduces a lot of uncertainty into the model inputs and consequently errors into the model output. For example, the $NO_2$ emissions were set as homogeneous across each of the separate emission volumes. In reality, however, vehicles do not drive in regular patterns. In addition, it is impossible to explicitly incorporate small obstacles in the studied street section (e.g. parked cars) into the model. Instead, their effects were taken into account by using a rough wall function. This, again, spreads their effect homogeneously over the studied street section, which is not true in reality.

One of the limitations of this study, is the limited number of simulated wind conditions, due to time limitations. It was observed that the selected wind conditions (directions SW and NW and approx. constant for one hour) probably occur frequently in reality at the studied site. However, it can be expected that the wind is also frequently more variable during the selected time of the day (rush hour, 17h00 – 18h00). Such scenarios are in need of further attention. Another limitation is the fact that the CFD model did not incorporate the effect of chemical reactions nor thermal effects. $NO_2$ is being used as main air pollutant and not $NO_x$ since NO is less toxic than $NO_x$. However, NO is unstable and forms $NO_2$ through photochemical oxidation. As a result of photolysis, $NO_2$ is converted back to NO, regenerating ozone ($O_3$). These reactions keep going until the equilibrium composition is reached (Soulhac et al., 2023). The study by Soulhac et al. (2023) indicates that in case of a busy street canyon, the photostationary equilibrium will not be fully achieved resulting in highly variable $NO_2$ concentrations. Even more, $NO_2$ concentrations will vary as a result of changes in the NO oxidation rate in response to $O_3$ variations (Brimblecombe et al., 2021) and in reality, photochemical reactions are far more complex and can be affected by volatile organic compounds (VOCs) as VOCs again affect $O_3$ concentrations and hereby change the reacting rates (Hang et al., 2022). These findings show that pedestrians are exposed to highly variable air pollution levels and that dispersion patterns of reactive pollutants are complex and unclear. The effect of these chemical reactions on computational model results is strongly disputed. Studies by Zhong et al. (2017), Hang et al. (2022) and Soulhac et al. (2023) emphasize that photochemistry should not be ignored. Furthermore, the study of Soulhac et al. (2023) showed that non-photostationary models bring significant improvements for modelling air pollution in street canyons. On the other hand, a number of counter arguments could be introduced which favor the use of photostationary models. Hang et al. (2022) conclude that the contribution of the VOCs chemistry to $NO_2$ concentrations is important for deep street canyons (AR = 5) due to the longer reaction time and is less relevant for regular street canyons (AR = 1), justifying the neglection of VOCs chemistry for the Belgiëlei model (AR ≈ 0.83). Brimblecombe et al. (2021) found that $O_3$ levels near pedestrian areas in street canyons may be limited, reducing the potential effect of NO oxidation. Even more, Santiago et al. (2017) concludes that under winter conditions, when the pollutant concentrations are less affected by atmospheric chemistry, the errors of using a photostationary model are neglectable (<15%). Laslty, it is clear that for simulations of complex urban environments (such as the Belgiëlei model or models used by Santiago et al. (2017) and Jeanjean et al. (2017)), it is customary to neglect chemical reactions due to computational limitations, whereas studies using complex chemistry (e.g. Zhong et al. (2017), Hang et al. (2022) and Soulhac et al. (2023)) mostly use simplified two-dimensional street canyon models. Due to the uncertain impact and the computational limitations, no atmospheric chemistry was introduced in the Belgiëlei model. However, the potential impact of chemical reaction should be borne in mind when interpreting the results of the $NO_2$ simulations.

Besides, due to computational issues, the simulation had to be stabilized using first order discretization for the convection of the turbulence variables, k and ε, and a total variation diminishing scheme for the convection of the other variables. Not applying full second order discretization, requires a higher grid resolution to achieve an acceptable accuracy in the solution. Consequently, it was not possible to achieve full grid convergence due to computational limitations. Still, the solution did not change qualitatively by using a finer grid and it can be expected that the large scale patterns observed in the obtained solutions (e.g. locations of high concentration areas) are of a high enough quality. In future research, we intend to resolve the problem of the discretization order of the current CFD model. Notwithstanding the mentioned limitations, CFD is still considered one of the most powerful and useful tools to predict pollution dispersion patterns (Lauriks et al., 2021).

Some limitations are also present regarding the input data for the CFD model. Traffic intensities were based on traffic counts from the 7th of July to the 6th of September 2021. However, these counts were performed whilst some COVID-19 restrictions were active. Therefore, it can be assumed that traffic intensities, and thus $NO_2$ emission, are higher in reality.

## 4. Conclusion

A comparative CFD study was conducted to investigate the effectiveness of adjusting traffic lane compositions combined with LBWs as a fast response tool to mitigate the exposure of pedestrians to traffic-related $NO_2$ emissions for a specific case study (Belgiëlei, Antwerp). Three scenarios were investigated: (1) the reduction of the number of traffic lanes (S01), the lateral displacement of all traffic lanes to the SE facade (S02) and the lateral displacement of traffic lanes to the NW facade (S03). In all scenarios, the effectiveness of adding low boundary walls (LBWs) was subsequently tested (S01 LBW, S02 LBW, S03 LBW). This study shows that displacing traffic lanes, and hereby altering the source-receptor pathways, may reduce exposure to $NO_2$ up to 8.0% on average in specific pedestrian zones. S02 LBW generated the largest general pedestrian exposure reduction to $NO_2$ of -3.6% (weighted average over the solution under NW and SW wind conditions) over the entire pedestrian area. On the other hand, S03 generated increased exposure levels (+1.0% over the entire pedestrian region and +8.0% on specific locations). This indicates that displacing traffic lanes might also affect pedestrian exposure to traffic-related air pollutants adversely, depending on the wind directions. LBWs were found to be efficient in further reducing the pedestrian exposure to $NO_2$. Even more, they were found to be a useful tool to mitigate the potentially adverse effect of lane displacements in case of the presence of less frequent wind directions.

In general it can be concluded that bundling pollution sources (compressing traffic lanes) and increasing the source-receptor distance (taking into account the in-canyon wind flow direction) is a valuable strategy to decrease pedestrian exposure to $NO_2$. Also, completed urban projects (e.g. the 24 hour transformation of St. Julian Street in Salzburg (Austria) or rapid transformation of traffic lanes to cycling lanes on Avenue Gabriel in Montreuil (France) during the COVID-19 pandemic) indicate that traffic lane adjustments are eligible as a fast-response strategy. Since the number of studies on the potential of alternating traffic lanes as a fast response tool for the reduction of pedestrian exposure to traffic-related pollutants is limited, it is suggested that further research is conducted on this matter. Hence the maximal reduction of 3.6%, the creation of $NO_2$ by NO oxidation may become more important as the distance between the source and the receptor increases. It is therefore suggested to conduct further research on this matter, which could be performed by the usage of an idealized street canyon model. Also, the impact of these interventions should be weighed against other interventions such as for example to introduction of strict emission-reduction strategies in order to provide well-considered advice for urban policy makers. Additionally, it is advised that the proposed interventions are applied in mock-up constructions and that their performance is tested and measured by conducting field studies, before applying them on a large scale in cities.

## References

Alphasense. (2022). Nitrogen Dioxide Sensors (NO2). Retrieved from https://www.alphasense.com/products/nitrogen-dioxide/

Ballari, M.M., & Brouwers, H.J.H. (2013). Full scale demonstration of air-purifying pavement. *Journal of Hazardous Materials, 254-255*, 406-414.

Blocken, B., Vervoort, R. , & van Hooff, T. . (2016). Reduction of outdoor particulate matter concentrations by local removal in semi-enclosed parking garages: A preliminary case study for Eindhoven city center. . *Journal of Wind Engineering and Industrial Aerodynamics, 159*, 80-98.

Boonen, Elia, & Beeldens, Anne. (2014). Recent Photocatalytic Applications for Air Purification in Belgium. *Coatings, 4*, 553-573.

Brimblecombe, P., Chu, M.Y., Liu, C.H., & Ning, Z. (2021). NOx and CO Fluctuations in a Busy Street Canyon. *Environments, 8*(137).

Buccolieri, R., Santiago, J.L., Rivas, E., & Sanchez, B. (2018). Review on urban tree modelling in cfd simulations: Aerodynamic, deposition and thermal effects. *Urban Forestry & Urban Greening, 31*, 212-220.

Chan, A.T., So, E.S.P., & Samad, S.C. (2001). Strategic guidelines for street canyon geometry to achieve sustainable straat air quality. *Atmospheric Environment, 35*, 4089-4098.

Chang, J.C., & Hanna, S.R. (2004). Air quality model performance evaluation. *Meteorology and Atmospheric Physics, 87*, 167-196.

City of Antwerp. (2006). *Strategisch ruimtelijk structuurplan Antwerpen*. Retrieved from https://www.antwerpen.be/info/540d92c9aea8a7ff428b4570/ruimtelijk-structuurplan-antwerpen

City of Antwerp. (2021). Stad in cijfers: Antwerpen. https://stadincijfers.antwerpen.be/dashboard/hoofd-dashboard/wonen

City of Antwerp. (2022). Opendata portaal Antwerpen. https://portaal-stadantwerpen.opendata.arcgis.com/datasets/boom/explore?location=51.208562%2C4.421692%2C19.00

City of Antwerp. (n.d.). *plaatsen van materialen of tijdelijke opstellingen op (of over) de openbare weg, openbaar domein of een publiek toegankelijk terrein*. Retrieved from https://www.antwerpen.be/docs/Stad/Bedrijven/Marketing_en_communicatie/MC_Com/evenementen/Evenementenaanvraag_documenten/verkortestandaardvoorwaarden.pdf

De Craemer, S., Vercauteren, J., Fierens, F., Lefebre, Wouter, Hooyberghs, H, & Meysman, F. (2019). *CurieuzeNeuzen: monitoring air quality together with 20.000 citizens*. Paper presented at the 40th AIVC - 8th TightVent - 6th venticool Conference, Ghent, Belgium.

EEA. (2021). Air quality standards. Retrieved from https://www.eea.europa.eu/themes/air/air-quality-concentrations/air-quality-standards

Frank, D.L., & Engelke, P. (2005). Multiple Impacts of the Built Environment on Public Health: Walkable places and the exposure to air pollution. *International Regional Science Review, 28*(2), 193-216.

Franke, J., Hellsten, A., Schlunzen, H., & Carissimo, B. (2007). *Best Practice Guideline for the CFD Simulation of Flows in the Urban Environment. Technical report*. Retrieved from https://www.researchgate.net/publication/257762102_Best_Practice_Guideline_for_the_CFD_Simulation_of_Flows_in_the_Urban_Environment_COST_Action_732_Quality_Assurance_and_Improvement_of_Microscale_Meteorological_Models

Geopunt Vlaanderen. (2020). DSI - Gewestplan, vector. https://www.geopunt.be/catalogus/datasetfolder/0c3ab5d8-2787-4db6-806c-8182d78a4a9b

Google. (n.d.). Google Earth Pro. Retrieved from https://earth.google.com/web/

Gromke, C., & Blocken, B. (2015). Inuence of avenue-trees on air quality at the urban neighborhood scale. part i: Quality assurance studies and turbulent schmidt number analysis for RANS CFD simulations. *Environmental Pollution, 196*, 214-223.

Hang, J., Liang, J., Wang, X., Zhang, X., Wu, L., & Shao, M. (2022). Investigation of O3–NOx–VOCs chemistry and pollutant dispersion in street canyons with various aspect ratios by CFD simulations. *Building and Environment, 226*, 109667.

Hassan, A.M., El Mokadem, A.A.F., Megahed, N.A., & Eleinen, O.M.A. (2020). Improving outdoor air quality based on building morphology: Numerical investigation. *Frontiers of Architectural Research, Article in press*.

Hauch, Andreas (Producer). (2010). Fairkehrtes Fest, blühende Strasse. Retrieved from https://urbangreens.tumblr.com/post/59877289605/jamesjgm-in-2010-salzburg-did-an-experiment/amp

Hofman, J., & Samson, R. (2014). Biomagnetic monitoring as a validation tool for local air quality models: A case study for an urban street canyon. *Environment International, 70*, 50-61.

Huang, Y.D., Hou, R.W., Liu, Z.Y., Song, Y., Cui, P.Y., & Kim, C.N. (2019). Effect of wind direction on the airflow and pollutant dispersion inside a long street canyon. *Aerosol and Air Quality Research, 19*, 1152-1171.

Huang, Y.D., Xu, X., & Kim, C.N. (2015). Effects of Strength and Position of Pollutant Source on Pollutant Dispersion Within an Urban Street Canyon. *Environmental Forensics, 16*, 163-172.
Huang, Y.D., Xu, X., Liu, Z.Y., Deng, J.T., & Kim, C.N. (2016). Impacts of shape and height of building roof on airflow and pollutant dispersion inside an isolated street canyon. *Environmental Forensics, 17*(4), 361-379.
Jeanjean, A.P.R., Gallagher, J., Monks, P.S., & Leigh, R.J. (2017). Ranking current and prospective NO2 pollution mitigation strategies: An environmental and economic modelling investigation in Oxford Street, London. *Environmental Pollution, 255*, 587-597.
Jicha, M., Pospisil, J., & Katolicky, J. (2000). Dispersion of pollutants in street canyon under traffic induced flow and turbulence. *Environmental Monitoring and Assessment, 65*, 343-351.
Kastner-Klein, P., & Plate, E.J. (1999). Wind- tunnel study of concentration fields in street canyons. *Atmospheric Environment, 33*, 3973-3979.
Katul, G.G., Mahrt, L., Poggi, D., & Sanz, C. (2004). One- and two-equation models for canopy turbulence. *Boundary-Layer Meteorology, 113*, 81-109.
Khomenko, S., Cirach, Marta, Pereira-Barboza, E., Mueller, N., Barrera-Gomez, J., Rojas-Rueda, D., . . . Nieuwenhuijsen, Mark. (2021). Premature mortality due to air pollution in European cities: a health impact assessment. *The Lancet Planetary Health, 5*(3), 121-134.
Lambrecht Meteo. (n.d.). products, wind. Retrieved from https://www.lambrecht.net/en/products/wind.html
Lauriks, T., Longo, R., Baetens, D., Derudi, M., Parente, A., Bellemans, A., . . . Denys, S. (2021). Application of Improved CFD Modeling for Prediction and Mitigation of Traffic-Related Air Pollution Hotspots in a Realistic Urban Street. *Atmospheric Environment, 246*(118127).
Liu, C.H., & Barth, M.C. (2002). Large-Eddy Simulation of Flow and Scalar Transport in a Modeled Street Canyon. *Journal of applied Meteorology, 41*, 660-673.
Llaguna-Munitxa, M., & Bou-Zeid , E. (2018). Shaping buildings to promote street ventilation: A large-eddy simulation study. *Urban Climate, 26*, 76-94.
Lovett, G.M. (1994). Atmospheric Deposition of Nutrients and Pollutants in North America: An Ecological Perspective. *Ecological Applications, 4*(4).
Maggos, Th., Plassais, A., Bartzis, J. G., Vasilakos, Ch., Moussiopoulos, N., & Bonafous, L. (2008). Photocatalytic degradation of NOx in a pilot street canyon configuration using TiO2-mortar panels. *Environ Monit Assess, 136*, 35-44.
McNabola, A., Broderick, B.M., & Gill, L.W. (2009). A numerical investigation of the impact of low boundary wallson pedestrian exposure to air pollutants inurban street canyons. *Science of the Total Environment, 407*, 760-769.
McNabola, A., O'Luanaigh, N., Gallagher, J., & Gill, L. (2013). The development and assessment of an aspiration efficiency reducing system of air pollution control for particulate matter in building ventilation systems. *Energy and Buildings, 61*, 177-184.
MetroCount. (2015). RoadPod VT. Retrieved from https://metrocount.com/products/roadpod-vehicle-tube-classifier/
Meysman, F.J.R., & De Craemer, S. (2018). *CurieuzeNeuzen Vlaanderen: Het cijferrapport*. Retrieved from https://static.standaard.be/Assets/Images_Upload/2018/09/28/CurieuzeNeuzen-Vlaanderen-rapport.pdf
Ming, T., Fang, W., Peng, C., Cai, C., de Richter, R., Ahmadi, M.H., & Wen, Y. (2018). Impacts of Traffic Tidal Flow on Pollutant Dispersion in a Non-Uniform Urban Street Canyon. *Atmosphere, 9*(3), 82-103.
Moradpour, M., Afshin, M., & Farhanieh, B. (2017). A numerical investigation of reactive air pollutant dispersion in urban street canyons with tree planting. *Atmospheric Pollution Research, 8*(2), 253-266.
Neophytou, M., Gowardhan, A., & Brown, M. (2011). An inter-comparison of three urban wind models using Oklahoma City Joint Urban 2003 wind field measurements. *Journal of Wind Engineering and Industrial Aerodynamics, 99*, 357-368.
NYC Department of Transportation. (2022). DOT Begins Work To Harden Protected Bike Lanes, Outlines Plan To Complete 20 Miles. Retrieved from https://www1.nyc.gov/html/dot/html/pr2022/begins-work-to-harden-protected-bike-lanes.shtml
Oke, T.R. (1988). Street design and urban canopy layer climate. *Energy and Buildings, 11*(1-3), 103-113.
Oke, T.R., Mills, G., Christen, A., & Voogt, J.A. (2017). *Urban Climates*. United Kingdom: Cambride University Press.
OpenFOAM. (2022). OpenFOAM. The OpenFOAM Foundation. Retrieved from https://openfoam.org/
OpenFOAM. (n.d.). C++ Source Code Guide. Retrieved from https://cpp.openfoam.org/v8/classFoam_1_1atmBoundaryLayer.html

OpenStreetMap. (n.d.). Transportkaart. Retrieved from https://www.openstreetmap.org/#map=13/51.2144/4.4193&layers=T

Park, S.J., Kim, J.J., Choi, W., Kim, E.R., Song, C.K., & Pardyjak, E.R. (2020). Flow Characteristics Around Step-Up Street Canyons with Various Building Aspect Ratios. *Boundary-Layer Meteorology, 174*, 411-431.

Parra, M.A., Santiago, J.L., Martin, F., Martilli, A., & Santamaria, J.M. (2010). A methodology to urban air quality assessment during large time periods of winter using computational fluid dynamic models. *Atmospheric Environment, 44*(17), 2089-2097.

Rijksoverheid. (2021). Emissiefactoren voor snelwegen en niet-snelwegen. Retrieved 18th of July 2022 https://www.rijksoverheid.nl/documenten/publicaties/2021/03/15/emissiefactoren-voor-snelwegen-en-niet-snelwegen-2021

Santiago, J.L., Borge, R., Martin, F., de la Paz, D., Martilli, A., Lumbreras, J., & Sanchez, B. (2017). Evaluation of a CFD-based approach to estimate pollutant distribution within a real urban canopy by means of passive samplers. *Science of the Total Environment, 576*, 46-58.

Sanz, C. (2003). A note on k - e modelling of vegetation canopy air-fows. *Boundary-Layer Meteorology, 108*, 191-197.

Soulhac, L., Fellini, S., Nguyen, V.C., & Salizzoni, P. (2023). Evaluation of Photostationary and Non-Photostationary Operational Models for Pollution in a Street Canyon. *Atmospheric Environment, 297*, 119589.

Spirn, Anne Whiston. (1986). *Air Quality at the Street--Level: Strategies for Urban Design.*, Harvard Graduate School of Design, Cambridge.

Tan, Z., Tan, M., Sui, X., Jiang, C., & Song, H. (2019). Impact of source shape on pollutant dispersion in a street canyon in different thermal stabilities. *Atmospheric Pollution Research, 10*, 1985-1993.

Telraam. (2020). Begliëlei Antwerpen. https://telraam.net/en/location/9000000828

Timmers, V., & Achten, P. (2016). Non-exhaust PM emissions from electric vehicles. *Atmospheric Environment, 134*, 10-17.

Tominaga, Y., & Stathopoulos, T. (2007). Turbulent Schmidt numbers for CFD analysis with various types of flow field. *Atmospheric Environment, 41*, 8091-8099.

van Druenen, T., van Hooff, T., Montazeri, H., & Blocken, B. (2019). CFD evaluation of building geometry modifications to reduce pedestrian-level wind speed. *Building and Environment, 163*, 106293.

Voordeckers, D., Lauriks, T., Denys, S., Billen, P., Tytgat, T., & Van Acker, Maarten. (2021a). Guidelines for passive control of traffic-related air pollution in street canyons: An overview for urban planning. *Landscape and Urban Planning, 207*, 103980.

Voordeckers, D., Meysman, F.J.R., Billen, P., Tytgat, T., & Van Acker, Maarten. (2021b). The impact of street canyon morphology and traffic volume on NO2 values in the street canyons of Antwerp. *Building and Environment, 197*, 107825.

Vos, E.J.P., Maiheu, Bino, Vankerkom, J., & Janssen, Stijn. (2013). Improving local air quality in cities: to tree or not to tree? *Environmental Pollution, 183*, 113-122.

WHO. (2013). *Review of evidence on health aspects of air pollution—REVIHAAP Project*. Retrieved from https://apps.who.int/iris/bitstream/handle/10665/341712/WHO-EURO-2013-4101-43860-61757-eng.pdf?sequence=1&isAllowed=y

WHO. (2016). *Ambient air pollution: A global assessment of exposure and burden of disease*. Retrieved from http://apps.who.int/iris/bitstream/handle/10665/250141/9789241511353-eng.pdf?sequence=1

Wieringa, J. (1992). Updating the Davenport roughness classi cation. *Journal of Wind Engineering and Industrial Aerodynamics, 41*(1-3), 357-368.

Xie, X., Huang, Z., & Wang, J.S. (2005). Impact of building configuration on air quality in street canyon. *Atmospheric Environment*(39), 4519-4530.

Yang, F., Gao, Y., Zhong, K., & Kang, Y. (2016). Impacts of cross-ventilation on the air quality in street canyons with different building arrangements. *Building and Environment, 104*, 1-12.

Zhang, K., Chen, G., Zhang, Y., Liu, S., Wang, X., Wang, B., & Hang, J. (2020). Integrated impacts of turbulent mixing and NOX-O3photochemistry onreactive pollutant dispersion and intake fraction in shallow and deepstreet canyons. *Science of the Total Environment, 712*, 1-24.

Zhong, J., Cai, X.M., & Bloss, W.J. (2017). Large eddy simulation of reactive pollutants in a deep urban street canyon: coupling dynamics with O3-NOx-VOC chemistry. *Environmental Pollution, 224*, 171-184.